

# Development of a Focused Library of Triazole-Linked Privileged-Structure-Based Conjugates Leading to the Discovery of Novel Phenotypic Hits against Protozoan Parasitic Infections

Elisa Uliassi,<sup>[a]</sup> Lorna Piazzini,<sup>[a]</sup> Federica Belluti,<sup>[a]</sup> Andrea Mazzanti,<sup>[b]</sup> Marcel Kaiser,<sup>[c, d]</sup> Reto Brun,<sup>[c, d]</sup> Carolina B. Moraes,<sup>[e, h]</sup> Lucio H. Freitas-Junior,<sup>[e, h]</sup> Sheraz Gul,<sup>[f]</sup> Maria Kuzikov,<sup>[f]</sup> Bernhard Ellinger,<sup>[f]</sup> Chiara Borsari,<sup>[g]</sup> Maria Paola Costi,<sup>[g]</sup> and Maria Laura Bolognesi<sup>\*,[a]</sup>

Protozoan infections caused by *Plasmodium*, *Leishmania*, and *Trypanosoma* spp. contribute significantly to the burden of infectious diseases worldwide, causing severe morbidity and mortality. The inadequacy of available treatments calls for cost- and time-effective drug discovery endeavors. To this end, we envisaged the triazole linkage of privileged structures as an effective drug design strategy to generate a focused library of high-quality compounds. The versatility of this approach was combined with the feasibility of a phenotypic assay, integrated with early ADME-tox profiling. Thus, an 18-membered library was efficiently assembled via Huisgen cycloaddition of phenothiazine, biphenyl, and phenylpiperazine scaffolds. The resulting 18 compounds were then tested against seven parasite strains, and counter-screened for selectivity against two mammalian cell lines. In parallel, *h*ERG and cytochrome P450 (CYP) inhibition, and mitochondrial toxicity were assessed. Remarkably, 10-((1-(3-((1,1'-biphenyl)-3-yloxy)propyl)-1*H*-1,2,3-triazol-5-yl)methyl)-10*H*-phenothiazine (**7**) and 10-(3-(1-(3-((1,1'-biphenyl)-3-yloxy)propyl)-1*H*-1,2,3-triazol-4-yl)propyl)-10*H*-phenothiazine (**12**) showed respective IC<sub>50</sub> values of 1.8 and 1.9 μg mL<sup>-1</sup> against *T. cruzi*, together with optimal selectivity. In particular, compound **7** showed a promising ADME-tox profile. Thus, hit **7** might be progressed as an antichagasic lead.

Infectious diseases caused by protozoan parasites pose a significant threat to human health, being responsible for more than a million deaths annually.<sup>[1]</sup> They also blight the lives of millions of people worldwide, affecting both the health and

economic stability of societies.<sup>[2]</sup> Malaria, leishmaniasis, and trypanosomiasis are three of the most important human protozoan diseases in terms of morbidity and mortality. For them, disability-adjusted life years, that is, the number of healthy life years lost to disability or premature death, is estimated to be in the millions.<sup>[3]</sup> While over 85% of deaths, disease, and disability occur in tropical and subtropical regions of the world, more temperate regions, including North America and Mediterranean Europe, are also impacted by protozoan diseases.<sup>[3]</sup> Nowadays, climate change and migration have added layers of complexity to the control of human protozoan infection. The enduring lack of an effective vaccine leaves chemotherapy as the only means to combat these diseases. However, most of the currently available medicines, which are decades old and suffer from low efficacy, high toxicity, and increasing resistance, by no means meet the clinical need. Therefore, the development of new pharmaceutical tools to treat protozoan diseases is now, more than ever, a global research priority.<sup>[4]</sup>

As for any therapeutic area, the identification of antiprotozoal new chemical entities can be undertaken using either phenotypic- or target-based approaches. Clearly, both approaches have advantages and disadvantages, which have been discussed in detail elsewhere.<sup>[5]</sup>

Due to improvements in cultivation and assay techniques of protozoa, phenotypic screening has become feasible in high-throughput mode, allowing screens of large compound collections. It has the intrinsic advantage of identifying compounds that are active in the whole-parasite context, thus cell-permeable, devoid of efflux issues and more likely to possess drug-like

[a] Dr. E. Uliassi, Dr. L. Piazzini, Dr. F. Belluti, Prof. M. L. Bolognesi  
Department of Pharmacy and Biotechnology, Alma Mater Studiorum—University of Bologna, Via Belmeloro 6, 40126 Bologna (Italy)  
E-mail: marialaura.bolognesi@unibo.it

[b] Prof. A. Mazzanti  
Department of Industrial Chemistry "Toso Montonari", Alma Mater Studiorum—University of Bologna, Viale del Risorgimento 4, 40136 Bologna (Italy)

[c] Dr. M. Kaiser, Prof. R. Brun  
Swiss Tropical and Public Health Institute, 4002 Basel (Switzerland)

[d] Dr. M. Kaiser, Prof. R. Brun  
University of Basel, Petersplatz 1, 4003 Basel (Switzerland)

[e] Dr. C. B. Moraes, Dr. L. H. Freitas-Junior  
Laboratório Nacional de Biociências (LNBio), Centro Nacional de Pesquisa em Energia e Materiais (CNPEM), 13083-100 Campinas (Brazil)

[f] Dr. S. Gul, M. Kuzikov, Dr. B. Ellinger  
Fraunhofer Institute for Molecular Biology and Applied Ecology Screening-Port, 22525 Hamburg (Germany)

[g] Dr. C. Borsari, Prof. M. P. Costi  
Department of Life Sciences, University of Modena and Reggio Emilia, Via Campi 103, 41125 Modena (Italy)

[h] Dr. C. B. Moraes, Dr. L. H. Freitas-Junior  
Present address: Instituto Butantan & Department of Microbiology, Institute of Biomedical Sciences, University of São Paulo, 05508-900 São Paulo (Brazil)

Supporting information and the ORCID identification number(s) for the author(s) of this article can be found under:  
<https://doi.org/10.1002/cmdc.201700786>.

features. Mammalian cell cytotoxicity assays are often run in parallel with parasite-based activity screens, allowing rapid elimination of compounds endowed with nonspecific cytotoxicity. However, unless one uses an appropriate genetically modified parasite that expresses readily detectable reporters, the identification of specific target(s) of active compounds is a necessary and complicated further step.<sup>[6]</sup>

For all these reasons, there has been a switch in emphasis to phenotypic approaches in antiprotozoal drug discovery research,<sup>[7]</sup> although target-based screening remains a major influence. Notably, several successful phenotypic campaigns have been reported in the areas of malaria, human African trypanosomiasis (HAT), and leishmaniasis, leading to clinical candidates.<sup>[5]</sup> Particularly, drug repurposing through phenotypic screening is a faster and more cost-effective method than de novo phenotypic approaches.<sup>[3]</sup> Clearly, this is an added value for the development of medicines against diseases endemic to low-income countries.

Along these lines, we sought a strategy that would meet the decreased cost and sustainability requirements of the field and tailored to our academic settings. Toward this goal, the use of validated chemical scaffolds emerged as a valuable option for assembling a focused chemical library.<sup>[8]</sup> It is widely recognized that chemical libraries enriched for certain “privileged” substructures are more likely to generate hits than randomly selected structures.<sup>[9]</sup> This is because such privileged substructures are structurally predisposed to binding efficiently to a wide range of targets.<sup>[10]</sup> In addition, their intrinsic drug-like properties offer an opportunity for providing leads with enhanced potential.<sup>[8a]</sup> Building on these considerations, for our library design (Figure 1), we selected three privileged substructures:



Figure 1. Design of a focused library of 4–21.

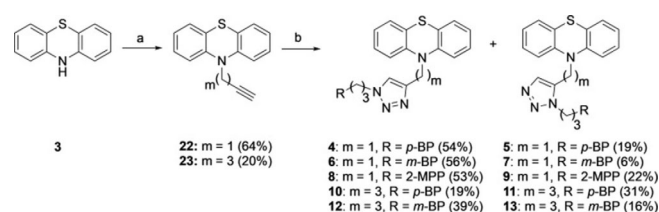
2-methoxyphenylpiperazine (2-MPP, 1), biphenyl (BP, 2), and phenothiazine (PTZ, 3).<sup>[11]</sup> Intriguingly, they have been largely explored,<sup>[12]</sup> but quite overlooked in the parasitic field. Although there are no reports of G protein coupled receptors (GPCRs) in kinetoplastids, the presence of 1, a classical GPCR-recognizing motif,<sup>[13]</sup> could enable probing the host–pathogen interactions as an indirect mechanism of action.<sup>[14]</sup>

Part of our strategy was to appropriately conjugate the selected privileged fragments ( $M_r < 200$  Da) covalently, giving rise to hit-like compounds ( $M_r \approx 500$  Da).<sup>[15]</sup> The ease of synthesis,

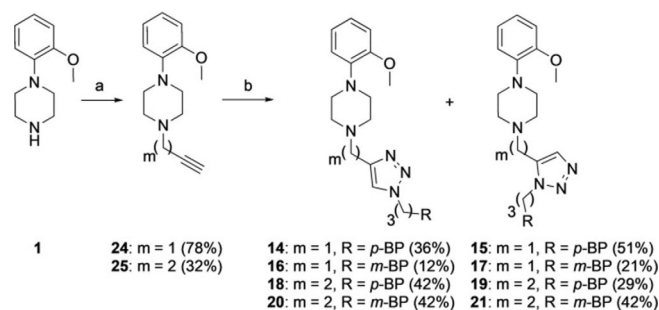
100% atom efficiency, and the high stability of the resulting 1,4- and 1,5-triazole products make the Huisgen cycloaddition ideally suited for this purpose. Furthermore, the triazole-connecting unit is a substructure present in several drug classes. On this basis, a focused library of compounds 4–21 was generated (Figure 1). To best of our knowledge, this is the first time that a rational design based on privileged structures combined with such a synthetic protocol has been proposed.

Next, a rapid in silico ADME-tox analysis was performed using QikProp (Table S1, Supporting Information).<sup>[16]</sup> Triazoles 4–21 were compliant for most of the computed descriptors ( $\leq 2$  violations), having properties that fell within the ADME-tox range of 95 % of known drugs. These data were supportive of the designed library drug-likeness.

Schemes 1 and 2 illustrate the simple and cost-effective synthesis of 4–21 by Huisgen reaction between the suitable alkyne (22–25) and azide (26–28) derivatives.

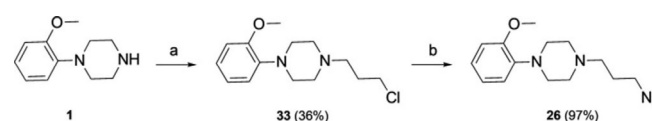


Scheme 1. Synthesis of 4–13: a) 29 or 30, KOTBu, DMSO, RT; b) selected azide (26–28), 64 °C.

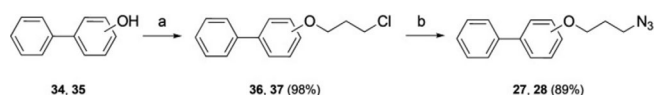


Scheme 2. Synthesis of 14–21: a) 29 or 31, KHCO<sub>3</sub>, toluene, reflux; b) selected azide (26–28), 64 °C.

Azides 26–28 were prepared by two consecutive nucleophilic substitution reactions, such that 1 was reacted with 1-bromo-3-chloropropane (32) in the presence of Et<sub>3</sub>N to afford 33, which was then quantitatively converted into the azide 26 (Scheme 3). On the other hand, Williamson reaction between *m*-hydroxybiphenyl (34) or *p*-hydroxybiphenyl (35) and 32



Scheme 3. Synthesis of 26: a) 32, Et<sub>3</sub>N, toluene, RT; b) NaN<sub>3</sub>, DMF, 60 °C.



**Scheme 4.** Synthesis of **27** and **28**: a) **32**,  $K_2CO_3$ , acetone, reflux; b)  $NaN_3$ , DMF, 60 °C.

gave **36** and **37**, which were subsequently transformed into the corresponding azides **27** and **28** (Scheme 4).

Alkynes **22** and **23** were respectively obtained by reacting **3** with 3-bromopropyne (**29**) and 5-chloro-1-pentyne (**30**) in the presence of  $KOtBu$  (Scheme 1), whereas **24** and **25** by holding **29** and **31** at reflux with  $KHCO_3$  (Scheme 2). Next, cycloaddition under solvent- and catalyst-free conditions afforded a mixture of 1,4- and 1,5-regioisomers of disubstituted 1,2,3-triazoles (**4–21**, 6–56% yields). The obtained regioisomers were easily purified, and their geometry was established by  $^1H$  NMR NOE spectroscopy experiments. In the case of the 1,4-disubstituted regioisomer, saturation of the  $CH_2$  protons at position 1 yielded NOE on the H-5 signal of triazole, and saturation of the second  $CH_2$  at position 4 yielded the same result, thus proving the spatial interaction between the above-mentioned protons. In the case of the 1,5-isomer, irradiation of the  $CH_2$  protons at position 1 of the triazole gave an enhancement of the  $CH_2$  protons at position 5 (Figures S1–S2, Supporting Information).

To investigate the therapeutic potential of **4–21**, we set up a screening pipeline against a panel of laboratory strains (Table 1). Thanks to a collaboration between New Medicines

for Trypanosomatidic Infections (NMTrypI)<sup>[17]</sup> and the Swiss Tropical and Public Health Institute (SwissTPHI),<sup>[18]</sup> seven parasite strains and two mammalian cell lines were exploited. In the case of HAT, the strains used were Lister 427 *Trypanosoma brucei brucei* (*T. b. brucei*), a cattle parasite, and STIB 900 *T. b. rhodesiense*, a human strain. Concerning Chagas disease (CD), the widely used Tulahuen clone and the Y strain of *T. cruzi* were selected. The panel also included *Leishmania infantum* (*L. infantum*) and *L. donovani*, two species responsible for serious visceral disease reported worldwide, including Mediterranean countries. Additionally, we chose the *Plasmodium falciparum* chloroquine- and pyrimethamine-resistant K1 (*P. falciparum* K1) strain, which is responsible for the most common multidrug-resistant malarial infections. Furthermore, to assess potential cytotoxic effects, studies were carried out on rat skeletal myoblast L6 cells and the human lung adenocarcinoma epithelial A549 cell line.

Table 1 lists the antiprotozoal and cytotoxicity profiles of **4–21**, together with the corresponding selectivity indices (SI). These results were analyzed according to the guidelines proposed by the Special Programme for Tropical Disease Research (TDR)<sup>[19]</sup> for early screening aimed to identify antiprotozoal hits.

With regard to *T. brucei*, only compounds **8** ( $IC_{50}$  *T. b. rhodesiense*: 2.3  $\mu g mL^{-1}$ , inhibition at 50  $\mu M$  *T. b. brucei*: 99.9%) and **19** ( $IC_{50}$  *T. b. rhodesiense*: 4.2  $\mu g mL^{-1}$ , inhibition at 50  $\mu M$  *T. b. brucei*: 95.2%) were found to inhibit both human and cattle strains. Nevertheless, **8** exhibited no or very little selectivity against mammalian cells (SI: 0.7 and 45% of A549 cell

**Table 1.** Antiprotozoal activities and cytotoxicities of compounds **4–21** in comparison with reference drugs.

Compound	<i>T. b. rhodesiense</i>		<i>T. cruzi</i> (Tulahuen)		<i>L. donovani</i>		<i>P. falciparum</i> K1		L6	Inhibition at 50 $\mu M$ [%]			A549 cell growth at 10 $\mu M$ [%]
	$IC_{50}$	SI <sup>[a]</sup>	$IC_{50}$	SI <sup>[a]</sup>	$IC_{50}$	SI <sup>[a]</sup>	$IC_{50}$	SI <sup>[a]</sup>		$IC_{50}$	<i>L. infantum</i> <sup>[b]</sup>	<i>T. b. brucei</i> <sup>[c]</sup>	
<b>4</b>	39.2	2.3	42.7	2.1	4.4	20.2	2.0	44.1	89.5	4.9	48.0	12.4	114.1
<b>5</b>	18.6	4.8	4.6	19.5	3.0	30.4	2.2	41.9	90.0	46.4	94.1	26.8	95.0
<b>6</b>	26.9	3.3	4.7	19.3	6.0	15.1	2.7	33.8	90.0	11.3	39.6	32.9	124.8
<b>7</b>	12.8	7.0	1.9	48.6	3.3	26.9	2.4	37.3	90.0	63.5	65.5	25.0	103.1
<b>8</b>	2.3	0.7	1.7	0.9	9.2	0.2	0.2	7.2	1.6	91.4	99.9	79.8	45.3
<b>9</b>	7.7	0.6	5.0	1.0	14.7	0.3	0.9	5.3	5.0	90.8	99.8	20.2	55.4
<b>10</b>	51.7	1.2	6.0	10.4	6.8	9.3	1.1	56.7	62.9	3.8	23.2	20.9	125.2
<b>11</b>	23.5	3.8	15.1	6.0	3.0	30.5	2.1	42.1	90.0	10.3	7.6	21.8	149.9
<b>12</b>	25.6	3.5	1.8	51.4	5.7	15.7	0.7	136.2	90.0	56.0	41.8	40.2	122.0
<b>13</b>	23.0	3.9	46.7	1.9	3.8	23.9	2.4	37.7	90.0	10.5	24.4	10.2	79.7
<b>14</b>	11.7	2.6	13.5	2.3	17.9	1.7	3.3	9.2	30.5	3.9	15.2	35.2	105.5
<b>15</b>	17.7	4.4	4.1	19.0	6.5	12.1	1.8	43.9	78.6	22.3	20.4	18.2	126.1
<b>16</b>	6.6	1.9	7.8	1.7	8.3	1.6	3.1	4.3	13.0	5.7	23.1	33.4	126.3
<b>17</b>	10.0	1.9	1.4	13.5	2.5	7.9	1.8	10.7	19.3	14.1	70.8	49.6	113.2
<b>18</b>	4.9	15.7	34.5	2.2	19.2	4.0	1.8	41.9	76.8	20.5	2.1	–4.8	87.5
<b>19</b>	4.2	18.0	6.7	11.2	11.9	6.3	1.6	46.6	75.1	35.6	95.2	–31.9	100.6
<b>20</b>	9.6	1.3	7.0	1.7	24.7	0.5	1.6	7.5	12.0	6.8	78.0	–59.5	99.2
<b>21</b>	4.0	1.7	3.9	1.7	13.9	0.5	0.3	22.6	6.9	68.5	39.5	17.2	121.7
melarsoprol	0.004	–	–	–	–	–	–	–	–	–	–	–	–
benznidazole	–	–	0.412	–	–	–	–	–	–	–	–	–	–
miltefosine	–	–	–	–	0.155	–	–	–	–	–	–	–	–
chloroquine	–	–	–	–	–	–	0.065	–	–	–	–	–	–
podophyllotoxin	–	–	–	–	–	–	–	–	0.004	–	–	–	–

The experimental errors of  $IC_{50}$  values [ $\mu g mL^{-1}$ ] are within  $\pm 50\%$ ; SD values of percent inhibition values agreed to  $\pm 10\%$ . [a] Selectivity index, calculated as ( $IC_{50}$  for L6)/( $IC_{50}$  for the respective parasite). [b] Amphotericin B ( $IC_{50} = 1.4 \mu g mL^{-1}$ ) was used as positive control for *L. infantum*. [c] Pentamidine ( $IC_{50} = 3.1 \mu g mL^{-1}$ ) was used as positive control for *T. b. brucei*. [d] Benznidazole ( $IC_{50} = 11.4 \mu g mL^{-1}$ ) was used as positive control for *T. cruzi* Y strain.

Table 2. In vitro early ADME-tox profiles of 4–21.<sup>[a]</sup>

Compound	% Inhibition hERG at 10 $\mu\text{M}$ $\pm$ STD %		% Inhibition CYP1A2 at 10 $\mu\text{M}$ $\pm$ STD %		% Inhibition CYP2C9 at 10 $\mu\text{M}$ $\pm$ STD %		% Inhibition CYP2C19 at 10 $\mu\text{M}$ $\pm$ STD %		% Inhibition CYP2D6 at 10 $\mu\text{M}$ $\pm$ STD %		% Inhibition CYP3A4 at 10 $\mu\text{M}$ $\pm$ STD %		% Mitochondrial viability at 10 $\mu\text{M}$ $\pm$ STD %	
4	34.71	9.78	32.53	4.70	40.07	7.97	53.60	4.10	16.74	3.44	61.26	3.10	74.79	0.81
5	58.40	23.97	30.59	1.95	33.52	6.23	67.47	3.43	54.93	1.67	59.86	5.13	110.11	11.65
6	33.61	22.22	32.22	2.20	50.17	1.70	54.24	4.90	18.54	4.45	63.17	4.23	110.75	19.83
7	17.38	6.91	47.01	0.79	27.16	4.31	81.08	2.75	39.95	2.68	61.12	4.74	124.25	10.84
8	88.67	5.95	23.49	5.13	58.82	2.90	45.13	5.93	81.88	2.57	89.29	0.92	132.80	7.86
9	88.31	6.79	30.34	4.21	42.61	3.17	54.58	3.21	99.56	1.29	85.41	2.67	126.61	12.27
10	24.88	14.25	27.79	1.29	64.67	0.98	94.90	1.19	29.19	4.12	73.20	2.30	98.77	23.19
11	37.55	13.31	30.41	3.20	57.04	3.08	89.01	1.64	30.95	3.47	72.47	4.51	85.83	25.94
12	39.81	12.48	44.05	2.66	74.54	3.32	91.89	1.67	71.82	1.67	85.03	1.61	82.47	16.57
13	47.86	16.62	46.88	4.40	49.16	3.52	97.08	1.70	55.87	1.63	83.45	1.46	84.37	6.82
14	96.20	6.28	22.51	4.70	67.66	4.16	70.79	1.72	105.34	0.65	91.09	0.68	135.68	8.93
15	34.40	8.24	27.59	2.56	93.04	0.83	73.03	2.99	69.80	2.34	91.44	2.10	126.95	14.11
16	89.29	12.35	25.88	4.34	49.06	5.06	59.83	4.24	102.28	0.35	85.37	2.41	122.71	9.19
17	42.96	13.42	25.46	2.42	84.15	1.29	77.50	1.98	75.72	1.63	95.80	0.58	117.93	24.09
18	100.17	9.10	24.59	4.21	72.99	0.97	59.76	3.71	101.41	3.36	80.75	1.72	137.02	14.89
19	75.53	10.16	33.92	2.85	79.52	2.22	74.96	3.04	90.67	1.12	92.01	0.42	117.94	13.9
20	102.28	11.63	23.48	5.37	78.70	2.96	68.33	0.53	100.53	0.34	82.82	1.55	136.33	14.08
21	62.79	16.99	31.00	5.74	63.31	3.26	78.02	2.02	93.91	2.52	71.59	3.22	118.17	18.92

<sup>[a]</sup> Traffic light legend

% inhibition of hERG and CYP isoforms: > 60%, > 30% < 60%, < 30%

% mitochondrial viability: < 0%, > 0 < 60%, > 60%

growth at 10  $\mu\text{M}$ ). Conversely, **19** was toxic only against L6 cells (SI: 18) and nontoxic against A549 cells (100% of cell growth). In addition, derivatives **18** and **21** yielded  $\text{IC}_{50}$  values of 4.9 and 4.0  $\mu\text{g mL}^{-1}$  against *T. b. rhodesiense*, despite modest (SI: 15.7) and poor (SI: 1.7) selectivity profiles against L6. Both compounds showed no cytotoxic effects on A549 cells at 10  $\mu\text{M}$ . Notably, **8**, **18**, **19**, and **21**, the only active derivatives of the library, feature a 2-MMP (**1**) substructure. However, none of them fulfilled the hit criteria for *T. b. rhodesiense* ( $\text{IC}_{50} < 0.2 \mu\text{g mL}^{-1}$ , and  $\text{SI} > 100$ ).<sup>[19]</sup>

An  $\text{IC}_{50}$  value of 1–2  $\mu\text{g mL}^{-1}$  and  $\text{SI} > 20$  were identified as requirements for *L. donovani* or *L. infantum*.<sup>[19]</sup> However, no hits were associated with such a profile. In addition to the very potent but highly cytotoxic compound **8** (see above), only **7**, bearing *m*-BP and PTZ substructures, resulted as a moderate inhibitor of both *Leishmania* forms ( $\text{IC}_{50}$  *L. donovani*: 3.3  $\mu\text{g mL}^{-1}$ , 63.5% inhibition of *L. infantum*), with a good safety profile (SI: 26.9 and 100% A549 cell growth at 10  $\mu\text{M}$ ).

Concerning *T. cruzi*, a broader range of activities against Tulahuen clone (1.7–46.7  $\mu\text{g mL}^{-1}$ ) was found, with clear structure–activity relationship patterns identified. As a general trend, with the exception of **9**, **11**, and **13**, we observed that 1,5-regioisomers (**5**, **7**, **15**, **17**, **19**, and **21**) are more active than the corresponding 1,4-isomers (**4**, **6**, **14**, **16**, **18**, and **20**). This reinforces the initial idea that the synthesis of both regioisomers would have expanded the chemical space explored by these compounds. Of note, several azoles have entered clinical trials for the treatment of CD.<sup>[20]</sup> Compounds **7** and **12**, which share the *m*-BP and PTZ substructures while differing in the

connecting methylene units, fully fulfilled the anti-*T. cruzi* hit requirements ( $\text{IC}_{50} < 2.0 \mu\text{g mL}^{-1}$ ,  $\text{SI} > 50$ ).<sup>[21]</sup> In fact, they show  $\text{IC}_{50}$  values for *T. cruzi* (Tulahuen) of 1.8 and 1.9  $\mu\text{g mL}^{-1}$ , along with promising SI values of 49 and 51, respectively. However, in the case of the *T. cruzi* Y clone, only the cytotoxic derivative **8** exhibited ~80% inhibition at 50  $\mu\text{M}$ , whereas all the others displayed percentages of inhibition below 49%. Correspondingly, the reference compound benznidazole displayed significantly different  $\text{IC}_{50}$  values against the two strains (Table 1). These discrepancies may be due to the use of different *T. cruzi* forms, but most probably because different assay setups were used (amastigotes in L6 cells and trypomastigotes co-seeded with human bone osteosarcoma epithelial cells, also covering intracellular amastigotes, respectively).<sup>[22]</sup>

Regarding *P. falciparum* K1, none of compounds **4**–**21** fully met the antimalarial hit criteria ( $\text{IC}_{50} < 0.2 \mu\text{g mL}^{-1}$ ,  $\text{SI} > 100$ ). However, **12**, which carries again BP and PTZ substructures, displayed potent antimalarial activity ( $\text{IC}_{50}$ : 0.7  $\mu\text{g mL}^{-1}$ ) and no sign of toxicity against mammalian cells (SI: 136 and 100% A549 cell growth at 10  $\mu\text{M}$ ).

Collectively, this early screening fostered the identification of **7** and **12** as promising trypanocidal hits against *T. cruzi* (Tulahuen), according to the TDR criteria.

In parallel, prioritization of **4**–**21** was not based solely on their antiprotozoal activities and selectivities, but focus was placed on investigating their in vitro early toxicity profiles<sup>[19]</sup> in terms of hERG and cytochrome P450 (CYP) inhibition, and mitochondrial toxicity (786-O, human renal carcinoma cell line) (Table 2). Compounds **4**–**21** were screened in each assay at

10  $\mu\text{M}$ , and a traffic light system was used, as previously reported.<sup>[23]</sup> Because azoles are well known for their CYP inhibitory activity, and significant inhibition of CYPs is a major cause of drug–drug interactions, especially in co-infected patients,<sup>[24]</sup> this emerged as a critical issue.<sup>[25]</sup> Indeed, among the five tested isoforms (CYP1A2, CYP2C9, CYP2C19, CYP2D6, and CYP3A4), CYP3A4 and CYP2C19 were inhibited by **4–21** to various extents. Notably, the anti-*T. cruzi* hit **7** was amongst the compounds associated with the least overall inhibition of the CYPs, while **12** was consistently more toxic. Perhaps the decreased flexibility of **7** with respect to **12**, together with the different triazole geometry is the reason for this behavior. With regards to *h*ERG inhibition, as this can induce cardiac toxicity, which must be avoided in pre-disposed CD patients,<sup>[26]</sup> unfortunately all the 2-MPP derivatives, with the exception of **15** and **17**, were associated with significant *h*ERG liability, whereas BP- and PTZ-based compounds (**4–7** and **10–13**) have modest *h*ERG liability. This is in agreement with QikProp prediction (Table S1). Intriguingly, when substructure **1** is linked to the triazole ring by one methylene unit, *h*ERG inhibition is not observed in the case of 1,5-regioisomers **15** and **17** with respect to the corresponding 1,4-isomers **14** and **16**.

Mitochondria are increasingly implicated in the etiology of drug-induced toxicities.<sup>[27]</sup> Accordingly, we tested whether **4–21** at 10  $\mu\text{M}$  could affect mitochondrial viability. Remarkably, all compounds displayed negligible mitochondrial toxicity.

Overall, the *in vitro* evaluation of early toxicity profile revealed some liabilities of **4–21**, which need to be addressed in further hit-to-lead optimization stages.

In summary, we established a panel of parasite/mammalian cell-based and early ADME-tox assays and screened a small focused library (compounds **4–21**) that was rapidly and efficiently assembled by combining three privileged substructures through a catalyst- and solvent-free Huisgen cycloaddition. When considering the TDR criteria,<sup>[19]</sup> we identified **7** (1,5-regioisomer) and **12** (1,4-regioisomer) as novel hits against *T. cruzi* that yield potent parasite growth inhibition, whilst being nontoxic to mammalian cells. Intriguingly, both **7** and **12** feature the *m*-BP and the PTZ substructures conjugated to the triazole through different methylene linkers. Although the *in vitro* early ADME-tox assessment highlighted potential metabolic liabilities for **12** (from moderate to significant inhibition against *h*ERG and all CYPs), positively, **7** inhibited only CYP3A4 and CYP2C19, with no *h*ERG and mitochondrial liability. Taken together, the new PTZ-triazole-*m*-BP chemotype represents an attractive starting point for further medicinal chemistry efforts aimed at developing new and sustainable antichagasic leads with an improved ADME-tox profile.

Importantly, the approach described herein might be a useful tool for antiprotozoal drug discovery: the multiple biological properties and the drug-likeness of privileged substructures together with the efficient triazole-based conjugation strategy foreshadow a huge variety of interesting conjugates yet to be explored.

## Acknowledgements

This work was supported by MIUR (PRIN Funds 201274BNKN\_003) and the University of Bologna (RFO 2016). Some antiparasitic activity and the early ADME-tox profiling were developed within the international collaborative effort of the European Union's Seventh Framework Programme for research, technological development and demonstration under grant agreement no. 603240 (NMTrypi—New Medicines for Trypanosomatidic Infections, <http://fp7-nmtrypi.eu/>).

## Conflict of interest

The authors declare no conflict of interest.

**Keywords:** phenotypic screening • privileged scaffolds • protozoan parasitic infections

- [1] J. R. Herricks, P. J. Hotez, V. Wanga, L. E. Coffeng, J. A. Haagsma, M. G. Basanez, G. Buckle, C. M. Budke, H. Carabin, E. M. Fèvre, T. Furst, Y. A. Halasa, C. H. King, M. E. Murdoch, K. D. Ramaiah, D. S. Shepard, W. A. Stolk, E. A. Undurraga, J. D. Stanaway, M. Naghavi, C. J. L. Murray, *PLoS Neglected Trop. Dis.* **2017**, *11*, e0005424.
- [2] P. J. Hotez, B. Pecoul, S. Rijal, C. Boehme, S. Aksoy, M. Malecela, R. Tapia-Conyer, J. C. Reeder, *PLoS Neglected Trop. Dis.* **2016**, *10*, e0003895.
- [3] K. T. Andrews, G. Fisher, T. S. Skinner-Adams, *Int. J. Parasitol. Drugs Drug Resist.* **2014**, *4*, 95–111.
- [4] L. Monzote, A. Siddiq, *Open Med. Chem. J.* **2011**, *5*, 1–3.
- [5] I. H. Gilbert, *J. Med. Chem.* **2013**, *56*, 7719–7726.
- [6] M. L. Sykes, V. M. Avery, *J. Med. Chem.* **2013**, *56*, 7727–7740.
- [7] A. Woodland, S. Thompson, L. A. Cleghorn, N. Norcross, M. De Rycker, R. Grimaldi, I. Hallyburton, B. Rao, S. Norval, L. Stojanovski, R. Brun, M. Kaiser, J. A. Frearson, D. W. Gray, P. G. Wyatt, K. D. Read, I. H. Gilbert, *ChemMedChem* **2015**, *10*, 1809–1820.
- [8] a) A. Cavalli, F. Lizzi, S. Bongarzone, F. Belluti, L. Piazza, M. L. Bolognesi, *FEMS Immunol. Med. Microbiol.* **2010**, *58*, 51–60; b) S. Bongarzone, M. L. Bolognesi, *Expert Opin. Drug Discovery* **2011**, *6*, 251–268.
- [9] K. L. Spear, S. P. Brown, *Drug Discovery Today Technol.* **2017**, *23*, 61–67.
- [10] P. M. Watt, *Future Med. Chem.* **2009**, *1*, 257–265.
- [11] E. Uliassi, L. Piazza, F. Belluti, M. Kaiser, R. Brun, S. Gul, B. Ellinger, C. B. Moraes, L. H. Freitas-Junior, C. Borsari, M. P. Costi, M. L. Bolognesi, *Proceedings* **2017**, *1*, 648.
- [12] a) D. A. Horton, G. T. Bourne, M. L. Smythe, *Chem. Rev.* **2003**, *103*, 893–930; b) A. Martinez, C. Gil in *Privileged Scaffolds in Medicinal Chemistry: Design, Synthesis Evaluation*, The Royal Society of Chemistry, London, **2016**, pp. 231–261.
- [13] T. A. Esbenshade in *G Protein-Coupled Receptors in Drug Discovery*, Vol. 4 (Eds.: K. H. Lundstrom, M. L. Chiu), CRC Press, Boca Raton, **2005**, pp. 15–36.
- [14] I. Pena, M. P. Manzano, J. Cantizani, A. Kessler, J. Alonso-Padilla, A. I. Bardera, E. Alvarez, G. Colmenarejo, I. Cotillo, I. Roquero, F. de Dios-Anton, V. Barroso, A. Rodriguez, D. W. Gray, M. Navarro, V. Kumar, A. Sherstnev, D. H. Drewry, J. R. Brown, J. M. Fiandor, J. J. Martin, *Sci. Rep.* **2015**, *5*, 8771.
- [15] C. A. Lipinski, *Drug Discovery Today Technol.* **2004**, *1*, 337–341.
- [16] Schrödinger Release 2017-4: QikProp, Schrödinger, LLC, New York, NY (USA), **2017**.
- [17] NMTrypi—New Medicines for Trypanosomatidic Infections: <http://fp7-nmtrypi.eu> (accessed November 30, 2017).
- [18] SwissTPHI—Swiss Tropical & Public Health Institute, Parasite Chemotherapy Unit: <https://www.swisstph.ch/en/> (accessed November 30, 2017).
- [19] S. Nwaka, B. Ramirez, R. Brun, L. Maes, F. Douglas, R. Ridley, *PLoS Neglected Trop. Dis.* **2009**, *3*, e440.

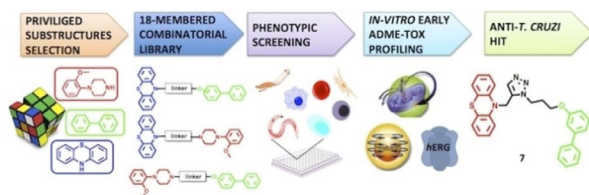
- [20] L. Gaspar, C. B. Moraes, L. H. Freitas, S. Ferrari, L. Costantino, M. P. Costi, R. P. Coron, T. K. Smith, J. L. Siqueira-Neto, J. H. McKerrow, A. Cordeiro-da-Silva, *Curr. Med. Chem.* **2015**, *22*, 4293–4312.
- [21] World Health Organization, *Chagas Disease: in vitro Screening Model*, [http://www.who.int/tdr/grants/workplans/en/chagas\\_invitro.pdf](http://www.who.int/tdr/grants/workplans/en/chagas_invitro.pdf) (accessed November 30, 2017).
- [22] C. B. Moraes, M. A. Giardini, H. Kim, C. H. Franco, A. M. Araujo, S. Schenkman, E. Chatelain, L. H. Freitas, *Sci. Rep.* **2014**, *4*, 4703.
- [23] E. Uliassi, G. Fiorani, R. L. Krauth-Siegel, C. Bergamini, R. Fato, G. Bianchini, J. C. Menendez, M. T. Molina, E. Lopez-Montero, F. Falchi, A. Cavalli, S. Gul, M. Kuzikov, B. Ellinger, G. Witt, C. B. Moraes, L. H. Freitas-Junior, C. Borsari, M. P. Costi, M. L. Bolognesi, *Eur. J. Med. Chem.* **2017**, *141*, 138–148.
- [24] a) E. Vaumourin, G. Vourc'h, P. Gasqui, M. Vayssier-Taussat, *Parasites Vectors* **2015**, *8*, 545; b) J. A. Lindoso, M. A. Cunha, I. T. Queiroz, C. H. Moreira, *HIV/AIDS* **2016**, *8*, 147–156.
- [25] K. Seden, S. Khoo, D. Back, N. Prevatt, M. Lamorde, P. Byakika-Kibwika, J. Mayito, M. Ryan, C. Merry, *AIDS* **2013**, *27*, 675–686.
- [26] F. S. Buckner, *Adv. Parasitol.* **2011**, *75*, 89–119.
- [27] J. A. Dykens, Y. Will, *Drug Discovery Today* **2007**, *12*, 777–785.

---

Manuscript received: December 15, 2017

Accepted manuscript online: ■■■■■, 0000

Version of record online: ■■■■■, 0000



An 18-membered library, rapidly and efficiently assembled by combining three privileged structures by catalyst- and solvent-free Huisgen cycloaddition, was screened in parasite/mammalian cell-based and early ADME-tox assays. Notably, compound **7** emerged as an

antichagasic phenotypic hit, with a good ADME-tox profile. The simple and versatile triazole-based conjugation strategy of privileged scaffolds might produce high-quality antiparasitic conjugates.

*E. Uliassi, L. Piazza, F. Belluti, A. Mazzanti, M. Kaiser, R. Brun, C. B. Moraes, L. H. Freitas-Junior, S. Gul, M. Kuzikov, B. Ellinger, C. Borsari, M. P. Costi, M. L. Bolognesi\**



**Development of a Focused Library of Triazole-Linked Privileged-Structure-Based Conjugates Leading to the Discovery of Novel Phenotypic Hits against Protozoan Parasitic Infections**

